Chapter 6
Microwave and Joule Heating Visualization by a Thermo-Elastic Microscope for Carbon Composite Materials

Sh. Arakelyan, A. Babajanyan, G. Berthiau, B. Friedman, and K. Lee

Abstract Microwave heating visualization for the carbon fiber/polyether ether ketone composite material was implemented using the thermo-elastic optical indicator microscopy (TEOIM) system. Losses of an anisotropic composite material were characterized due to the microwave radiation influence. TEOIM visualization showed that the near-field distribution stretches along the composite material high conductivity axis and takes different forms when some defects in the composite material were analyzed.The visualized microwave heat was measured to be 0.2 K when the probe feeding power was around 15 dBm.The Obtained microwave heat visualization data was in good agreement with the simulated result. Additionally, noninvasive Joule heating (around 1 K) made by 0.3 A DC flux was observed in order to characterize mechanical faults in a composite material.

6.1 Introduction

Reinforced carbon fiber composites have wide range of applications in medicine (surgical and dental pharmaceutical applications), aircraft construction, engineering, industry, etc. [1–4]. The carbon fibers are stable under high mechanical stress, have refined elastic properties and can resist high mechanical deformation by changing shape whereas other materials such as metals or ceramics would be destroyed. In some applications, carbon fibers composite materials can successfully replace metals [5]. Depending on the required properties carbon fibers with various structural com-

Sh. Arakelyan · K. Lee
Department of Physics, Sogang University, Seoul 121-742, Korea

A. Babajanyan (✉)
Department of Radiophysics, Yerevan State University, Yerevan 0025, Armenia
e-mail: barsen@ysu.am

G. Berthiau
IREENA, Boulevard de L'iniversite 37, BP-406, 44602, Saint-Nazaire Cedex, France

B. Friedman
Department of Physics, Sam Houston State University, Huntsville, TX 77341, USA

D. Blaschke et al. (eds.), *Optics and Its Applications*, Springer Proceedings in Physics 281, https://doi.org/10.1007/978-3-031-11287-4_6

binations are used. An example of such a fiber configuration is a unidirectional carbon fiber/polyether ether ketone (PEEK) composite material, the mechanical properties of which are well studied [6–8].

Due to its nature the electrical and mechanical properties of the carbon fiber/PEEK composite material are spatially anisotropic. Such anisotropic properties are attractive from the point of view material science particularly, when investigating the interaction between the electromagnetic field and a material. Recent examples of such studies include: microwave absorption properties investigation [9, 10] and its enhancement for radar absorption purposes [11, 12], carbon-based composites mechanical properties enhancement by microwave curing [13, 14], characterization of anisotropic electrical properties of a carbon fiber/PEEK composite [15], testing and inspection of reinforced carbon composites by a microwave microscopy [16] etc. The heating process due to the microwave absorption is important in the above studies and thus we have undertaken a detailed investigation. In the heating of high electrical conductivity materials induction currents are responsible whereas for low conductivity materials the heat generally is created due to displacement currents [17, 18]. From this point of view, the investigation of composite material anisotropy properties presents a wide area of interest, since the anisotropic electrical conductivity of the unidirectional carbon fiber/PEEK composite material is drastically changed depending on the fibers orientation. However, to characterize the microwave heating mechanisms and losses in the composite material one must use temperature detection systems with a high sensitivity. An example of such a system is the thermo-elastic optical indicator microscopy (TEOIM) technique developed by H. Lee and co-authors for the temperature and microwave near-field visualization [19]. The TEOIM technique with slide glass indicators visualizes the thermal distribution without a scanning process and is more sensitive (up to 4 mK) compared to other thermal detectors such as infrared devices [20, 21].

In this paper, we present microwave energy losses characterization in carbon fibers/PEEK composite material by the TEOIM visualization. We visualize microwave heating of the composite material sheet and observe its changes when artificial defects in the form of hole have been made in a composite material sheet. We also provide a COMSOL Multiphysics simulation for the best understanding of the anisotropic material heating phenomenon and comparable analysis of obtained experimental results. Taking into account the thermal distributions due to the conductive and dielectric losses it will be possible to realize a qualitative estimation of the electromagnetic field distribution. In addition, to characterize mechanical defects in a composite material we perform Joule heat visualization caused by a direct current (DC) flux. The proposed defect measurement technique may become a supplement to the mechanical property testing used for carbon fiber reinforced composites. Such investigation may also be a useful tool for the study of electromagnetic shielding properties in an anisotropic material.

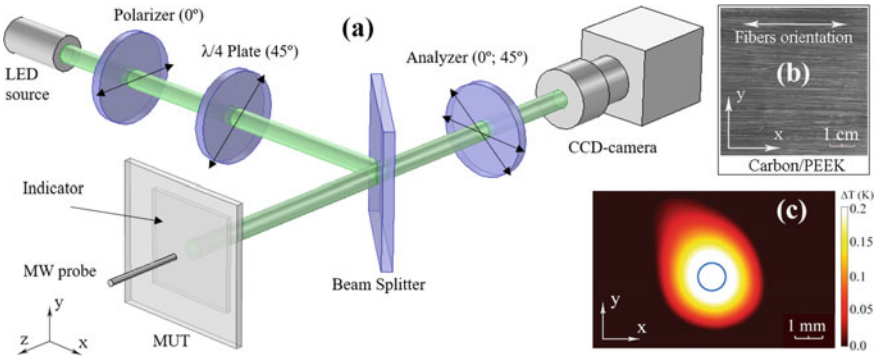

Fig. 6.1 **a** The experimental setup of the thermo-elastic imaging system, **b** the fibers orientation in the composite material, and **c** the visualized thermal pattern caused by microwave field at 5 GHz from end of MW probe at 1 cm distance

6.2 Materials and Methods

The temperature distribution in a material with electrical and thermal anisotropy was measured by the TEOIM technique [19]; a schematic diagram is shown in Fig. 6.1a.

The composite material with 6 cm × 6 cm surface area used in our experiments consists of PEEK and unidirectional aligned carbon fibers with diameters of 1 μm Fig. 6.1b. The volume fraction of fibers in the composite material is 3 : 5 (or 60%). The electrical and thermal conductivities of the composite sheet are diagonal tensors with elements of $\sigma_{xx} \cong 3.9 \times 10^4 S/m$, $\sigma_{yy} = \sigma_{zz} \cong 7.7 S/m$ [22] and $k_{xx} \cong 4.5 W/(m \cdot K)$, $k_{yy} = k_{zz} \cong 0.67 W/(m \cdot K)$ [23] respectively. In all experiments, composite material fibers were aligned along the x-axis. As an indicator, we have used a borosilicate glass substrate (Corning Eagle XG) with a 200 nm Pt deposited layer. Indicator has 4 cm × 4 cm sizes and placed at distance of 5 mm from sample. An Agilent E5071B network analyzer in the continuous mode was used as a power source for feeding of a microwave (MW) probe with diameter of 1 mm. All measurements were performed by a microwave signal with 15 dBm power and 5 GHz frequency at 1 cm distance from sample. The visualized thermal distribution (without sample) caused by microwaves at 5 GHz and at 1 cm distance from MW probe end is presented in Fig. 6.1c. For Joule heating measurements, an HP E3631A programmable DC power supply has replaced the network analyzer. A reliable contact on the carbon fiber/PEEK sheet has been provided by using a silver paste on the composite material edges, alight emitted diode ($\lambda = 530$ nm) matrix was used as a light source, a polarizer and a quarter-wave plate provide the circular polarized light incidence on the indicator film as shown in the Fig. 6.1a configuration. By a beam splitter the circular polarized light is being directed to the indicator, then during the reflection from the indicator the light polarization state is being changed to elliptical due to the mechanical stresses in the indicator and recorded by CCD camera with resolution of 1024 × 640.

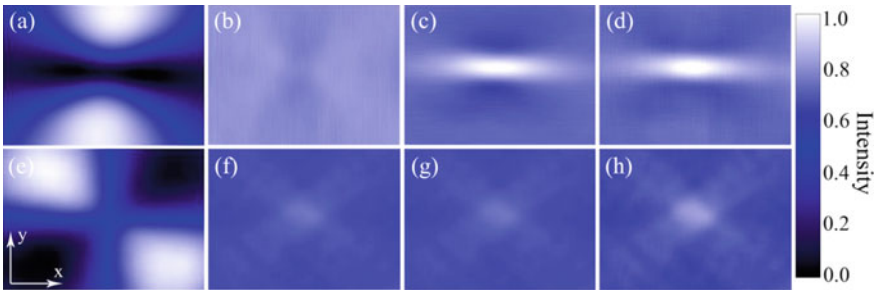

Fig. 6.2 Image-processing steps in LabVIEW: **a** and **e** correspond to the measured β_1 and β_2 images, respectively; **b** and **c** are $d^2\beta_1/dx^2$ and $-d^2\beta_1/dy^2$, respectively; **f** and **g** are $d^2\beta_2/dxdy$ and $d^2\beta_2/dydx$, respectively. **d** and **h** represent (**b**)+(**c**) and (**f**)+(**g**), respectively. The final obtained image is the sum of (**d**) and (**h**)

During the measurements the analyzer orientation has been changed to be 0° or 45° with respect to the xy-plane and by choosing the corresponding orientation of the analyzer the charge-coupled device (CCD)-camera detects mechanical stress distribution images (β_1 and β_2). For the temperature distribution calculation, we solved the inverse problem of mechanical stress formation caused by the heat in a thin indicator film. The solution of that inverse problem i.e. the relation between the heat source density and mechanical stress distributions has the following form

$$q = C\left(\frac{\partial^2\beta_1}{\partial x^2} - \frac{\partial^2\beta_2}{\partial y^2} + 2\frac{\partial^2\beta_2}{\partial x\partial y}\right), \tag{6.1}$$

where q is the heat source density, β_1 and β_2 are linear birefringent distribution images corresponding to 0° and 45° of the analyzer orientation, and C is the constant related to the indicator parameters and the wavelength of the probing light.

Figure 6.2 illustrates image processing steps corresponding to the measured mechanical stress distributions. As Eq. (6.1) shows the obtained final image will be (b) + (c) + (f) + (g) which will represent the temperature difference between two states i.e. in the presence and absence of the heat source. More details about the visualization technique used and image processing are described in [19].

6.3 Results and Discussion

One should take into consideration the microwave loss mechanisms in a material to understand the origin of microwave heating. Since the carbon/PEEK does not have magnetic losses the losses due to the imaginary part of the relative permeability can be neglected. Thus in a composite material heating, the conductive and dielectric losses are responsible [18]. In our experiment, at the microwave probe apex the

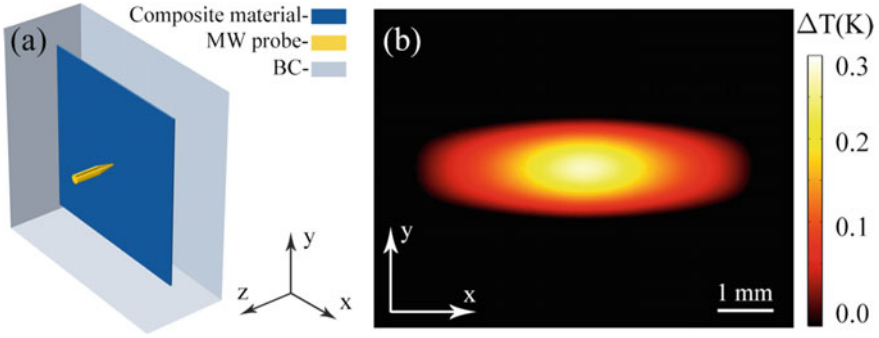

Fig. 6.3 COMSOL Multiphysics simulation: **a** geometry of the model with indications of MW probe and boundary condition (BC), **b** simulated microwave heat distribution in the carbon/PEEK

electromagnetic near-field symmetry following to the symmetry of its geometry; the electric field is concentrated around the probe head area whereas the magnetic field intensity is zero in that area due to eddy behavior. When the composite sheet is placed close to the microwave probe, the field symmetry is stretched along the high conductivity axis and the field distribution becomes elliptical. The induced current in the composite material leads heating of the sample.

We modeled the carbon fiber/PEEK microwave heating in COMSOL Multiphysics interface to compare obtained experimental data with the theoretical model. The geometry of the simulated microwave heating is shown in Fig. 6.3a. The model was built by the multiphysical coupling of two modules: the "Electromagnetic Wave" and "Heat Transfer in Solids". In the model, we used "Coaxial Lumped Port" with power of 15 dBm as a microwave source for the probe feeding, we set "Scattering" and "Temperature" boundary conditions for the "Electromagnetic Wave" and "Heat Transfer in Solids" modules, respectively, and configured the "Frequency Domain" and "Stationary" solvers for them. Thermal and electrical conductivities of the carbon/PEEK were set corresponding to the data mentioned in section "Material and Methods", 1320 kg/m^3 and 6 J(kg · K) were chosen as a density and heat capacity respectively, air was taken as an ambient environment, and the microwave probe was set to be perfect electric conductor. The simulation result is shown in Fig. 6.3b where the elliptic distribution is caused by the anisotropy of thermal and electrical conductivities, since the induced current flows easily through the high electrical conductivity direction and the largest portion of its generated heat transfers along the same direction.

Figure 6.4a shows the microwave heat distribution in the carbon fiber/PEEK visualized by the TEOIM technique. Here the orientation of the ellipse foci coincides with the high electrical conductivity direction as it was theoretically assumed and simulated above. Note that the 0.1 K of difference of the simulated and measured heat magnitude may be caused by choosing the microwave probe as a perfect conductor or some material properties mismatch. By varying simulation parameters one can perfectly match the experimental and simulated results, however we skip that since

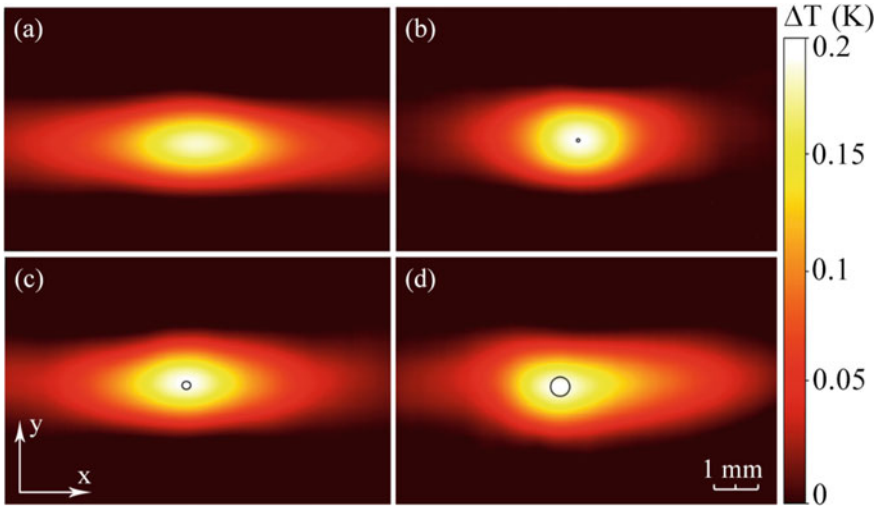

Fig. 6.4 Measured images for microwave heating distribution in the carbon/PEEK: **a** defect-free sample and sample with defect diameters of **b** 0.1 mm, **c** 0.2 mm, and **d** 0.4 mm

the simulated model initially has been built for the qualitative understanding of the microwave heat origin in the carbon fibers/PEEK. We made some artificial defects in the composite material in order to observe the heat distribution changes caused by defects. We varied the diameter of circle shaped hole type defects in the range of 0.1–0.4 mm.

As shown in Fig. 6.4b–d the hole in the center of the sample changes the heat distribution. One can see that even for the smallest defect size (0.1 mm) the shape of the visualized heat distribution has shrunken along the high conductivity direction. The reason for such shrinking phenomenon is that the defect interrupts the carbon fibers continuity and leads to the changes of the induced current distribution around the defect location. Depending on the growth of the defect size the changes in the heat distribution become more important. The image asymmetry in Fig. 6.4d comes from the position of the microwave probe with respect to the hole center. The symmetry in the resulting image was drastically changed only when the defect size was more than the microwave probe size (0.1 mm). Summarizing the microwave heat visualizations, we claim that fabrication faults and defects in a composite material sheet can be discovered by the microwave heating visualization and comparison of defect-free and custom/testing samples.

Figure 6.5 shows the Joule heat visualization for the defective carbon/PEEK composite material when the DC flux has been 0.3 A. Note that along the high electrical conductivity direction the Young's modulus (a measure of the stiffness) also is high, that is to say the mechanical defect can be discovered by the Joule heating visualization. In Fig. 6.5b high intensities correspond to the areas where the high electrical conductivity was interrupted by the defects. Those areas represent themselves the

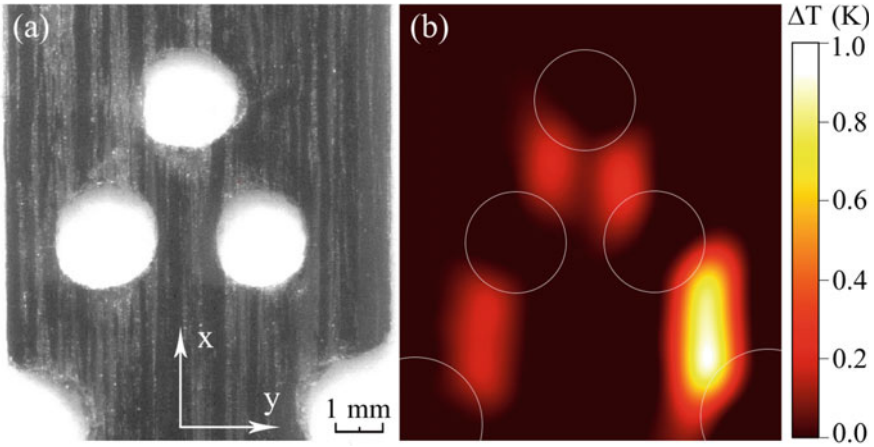

Fig. 6.5 **a** Optical image and **b** heat distribution visualization of the defective carbon/PEEK sample under the 0.3 A DC flux

mechanical defect areas. In this experiment the diameters of defective holes were around 2 mm which simply could be observed by the CCD camera without applying any heat visualization technique. However, in many cases optical observation is impossible e.g. when the defect is located inside of the material or when it is too small for the CCD camera observation. Note that the spatial resolution of the TEOIM technique is around 200 nm [19] which makes possible even single fiber defect detection. Since the system works as polarization microscope, the TEOIM sensitivity and spatial resolution caused by ability of high accuracy polarization detection and CCD camera pixel density, as well as data processing but not by optical light intensity and wavelength. We used linear polarized green light (530 nm) but similar measurement accuracy provided using a blue light (400 nm) and even white light sources. We suggest that this technique can be applied successfully for non-destructive testing and examination purposes.

6.4 Conclusion

The loss properties investigation for the carbon/PEEK composite material was performed by microwave heat visualization. The described loss mechanisms for microwave power give information about the heat mapping which can be used for material defect characterization and discovery. We succeeded in visualizing microwave and Joule heat in a carbon fiber/PEEK composite material.

Taking into account that this visualization technique is appropriate for investigations of DC and microwave influence on the composite material, we assert that this

technique can be a promise tool for nondestructive testing and analysis during design and fabrication processes.

Acknowledgements This work was supported under the framework of international cooperation program managed by National Research Foundation of Korea (NRF-2020K2A9A2A08000165, FY2021) and funded by the Korea government (MSIT) (NRF-2021R1A2C1007334), by a scientific research grant through the Science Committee of MESCS of Armenia (21AG-1C061) and by a faculty research funding program 2021 implemented by Enterprise Incubator Foundation with the support of PMI Science.

References

1. Harris, B.: Engineering Composite Materials. IOM (1999)
2. Gruner, G.: Carbon nanotube films for transparent and plastic electronics. J. Mater. Chem. **16**, 3533 (2006)
3. Saiello, S., Kenny, J., Nicolais, L.: Interface morphology of carbon fibre/PEEK composites. J. Mater. Sci. **25**, 3493–3496 (1990)
4. Lonjon, A., Demont, P., Dantras, E., et al.: Electrical conductivity improvement of aeronautical carbon fiber reinforced polyepoxy composites by insertion of carbon nanotubes. J. Non Cryst. Solids **358**, 1859–1862 (2012)
5. Kadirvelu, K., Thamaraiselvi, K., Namasivayam, C.: Removal of heavy metals from industrial wastewaters by adsorption onto activated carbon prepared from an agricultural solid waste. Bioresour. Technol. **76**, 63–65 (2001)
6. Wang, H., Vu-Khanh, T.: Damage extension in carbon Fiber/PEEK Crossply laminates under low velocity impact. J. Compos. Mater. **28**, 684–707 (1994)
7. Qiang Yuan, Q., Bateman, S.A., Friedrich, K.: Thermal and mechanical properties of PAN- and Pitch-based carbon fiber reinforced PEEK composites. J. Thermoplast. Compos. Mater. **21**, 323–336 (2008)
8. Curson, A.D., Leach, D.C., Moore, D.R.: Impact failure mechanisms in carbon Fiber/PEEK Composites. J. Thermoplast. Compos. Mater. **3**, 24–31 (1990)
9. Liu, L., Zhou, K., He, P., et al.: Synthesis and microwave absorption properties of carbon coil-carbon fiber hybrid materials. Mater. Lett. **110**, 76–79 (2013)
10. Choi, J., Jung, H.-T.: A new triple-layered composite for high-performance broadband microwave absorption. Compos. Struct. **122**, 166–171 (2015)
11. Neo, C.P., Varadan, V.K.: Optimization of carbon fiber composite for microwave absorber. IEEE Trans. Electromagn. Compat. **46**, 102–106 (2004)
12. Zang, Y., Xia, S., Li, L., et al.: Microwave absorption enhancement of rectangular activated carbon fibers screen composites. Compos. Part B Eng. **77**, 371–378 (2015)
13. Xu, X., Wang, X., Cai, Q., et al.: Improvement of the compressive strength of carbon fiber/epoxy composites via microwave curing. J. Mater. Sci. Technol. **32**, 226–232 (2016)
14. Lee, H.S., Kim, S., Noh, Y.J., et al.: Design of microwave plasma and enhanced mechanical properties of thermoplastic composites reinforced with microwave plasma-treated carbon fiber fabric. Compos. Part B Eng. **60**, 621–626 (2014)
15. Lee, H., Galstyan, O., Babajanyan, A., et al.: Characterization of anisotropic electrical conductivity of carbon fiber composite materials by a microwave probe pumping technique. J. Compos. Mater. **50**, 1999–2004 (2015)
16. Rufail, L., Laurin, J.-J., Moupfouma, F.: On the use of microwave microscopy for detecting defects in the lightning strike protection mesh for carbon fiber composite aircraft. In: 2016 17th International Symposium on Antenna Technology and Applied Electromagnetics (ANTEM). IEEE, pp. 1–2

17. Bailleul, M.: Shielding of the electromagnetic field of a coplanar waveguide by a metal film: Implications for broadband ferromagnetic resonance measurements. Appl. Phys. Lett. **103**, 192405 (2013)
18. Mekhitarian, V.M.: The Faraday law of induction for an arbitrarily moving charge. J. Contemp. Phys. (Armenian Acad. Sci.) **51**, 108–126 (2016)
19. Lee, H., Arakelyan, S., Friedman, B., et al.: Temperature and microwave near field imaging by thermo-elastic optical indicator microscopy. Sci. Rep. **6**, 39696 (2016)
20. Pris, A.D., Utturkar, Y., Surman, C., et al.: Towards high-speed imaging of infrared photons with bio-inspired nanoarchitectures. Nat Photonics **6**, 564–564 (2012)
21. LeMieux, M.C., McConney, M.E., Lin, Y.-H., et al.: Polymeric nanolayers as actuators for ultrasensitive thermal bimorphs. Nano Lett. **6**, 730–734 (2006)
22. Bui, H.K., Wasselynck, G., Trichet, D., et al.: 3-D modeling of thermo inductive non destructive testing method applied to multilayer composite. IEEE Trans. Magn. **49**, 1949–1952 (2013)
23. Pan, C.T., Hocheng, H.: Evaluation of anisotropic thermal conductivity for unidirectional FRP in laser machining. Compos. Part A Appl. Sci. Manuf. **32**, 1657–1667 (2001)